Additional soft jets in $t\bar{t}$ production at the Fermilab Tevatron $p\bar{p}$ collider

Lynne H. Orr

Department of Physics, University of Rochester, Rochester, New York 14627-0171

W.J. Stirling

Departments of Physics and Mathematical Sciences, University of Durham, Durham DH1 3LE, England
(Received 2 September 1994)

A large fraction of top quark events in $p\bar{p}$ collisions at 1.8 TeV will contain additional soft hadronic jets from gluon bremsstrahlung off the quarks and gluons in the hard processes $q\bar{q}, gg \rightarrow t\bar{t} \rightarrow b\bar{b}W^+W^-$. These extra jets can cause complications when attempting to reconstruct m_t from the invariant mass of combinations of final-state quarks and leptons. We show how such soft radiation cannot be unambiguously associated with either initial-state radiation or with final-state radiation off the b quarks. The top quarks can radiate too, and in fact the pattern of radiation has a very rich structure, which depends on the orientation of the final-state particles with respect to each other and with respect to the beam. We calculate the full radiation pattern of soft jets in the soft gluon approximation and compare with several approximate forms which are characteristic of parton shower Monte Carlo simulations. The implications for top mass measurements are discussed.

PACS number(s): 14.65.Ha, 13.85.Qk, 13.87.−a, 14.70.Dj

I. INTRODUCTION

Very recently the Collider Detector at Fermilab (CDF) Collaboration has reported evidence for a top quark of mass 174 ± 17 GeV/c^2 in $p\bar{p}$ collisions at 1.8 TeV [1]. The leading-order production processes are $q\bar{q}, gg \rightarrow t\bar{t} \rightarrow b\bar{b}W^+W^-$, and a statistically significant signal is seen in the channels $W^+W^- \rightarrow l\nu l\nu$ and $W^+W^- \rightarrow l\nu$ + jets ($l = e, \mu$). From the latter sample, the top mass is reconstructed from the final-state lepton and jet momenta. A potential problem with this procedure arises when the final state contains an additional hadronic jet, since it is not known *a priori* whether this jet arises from initial-state radiation, in which case it should be ignored, or whether it originated (say) in bremsstrahlung off a b quark, in which case it should be included in the m_t reconstruction. We note that a substantial fraction of the candidate top events reported by CDF do indeed have an additional jet over and above the number associated with the leading-order production and decay process.

In fact there is *no* meaningful separation of such jets into "initial-" and "final-state" radiation [2]. In any part of phase space, the soft jet cross section contains contributions from radiation off the incoming $q\bar{q}, gg$, off the produced $t\bar{t}$ at the production stage, off the t and b quarks in the $t \rightarrow bW$ decay process, and from interferences between these. In specific regions, however, we might expect certain types of radiation to be more important than others. For example, we would expect radiation close to the beam axis to be dominated by gluon emission off the incoming partons, while radiation close to a b quark should be dominated by collinear gluon emission off that quark. But away from these special collinear regions, all particles (including the top quarks) emit gluons with approximately equal strength. In what follows, we will study the distribution of soft gluon radiation over all

of phase space, to see to what extent our expectations about initial- and final-state radiation are valid. We will see that while the initial- and/or final-state radiation picture is too naïve, a decomposition of the radiation pattern into contributions associated with $t\bar{t}$ production, decay, and their interference provides the information necessary for top mass reconstruction.

Our purpose in this paper is twofold. First, we wish to study the correct distributions[1] to determine where the gluons come from and where they go, in a way that is directly relevant to top momentum reconstruction and mass measurement. Our second aim is to compare these results with simpler models which are characteristic of the way gluon radiation is implemented in Monte Carlo event generators, such as the initial- and/or final-state picture mentioned above. The difference between these approximations and the exact treatment could then provide an indication of the errors implicit in using certain Monte Carlo simulations to generate extra soft jets in $t\bar{t}$ production.

II. GENERAL FORMALISM FOR SOFT GLUON RADIATION

A. Gluon radiation in $t\bar{t}$ production and decay

We start with the leading-order process

$$a(k_1) + b(k_2) \rightarrow t(q_1) + \bar{t}(q_2) \rightarrow b(p_1) + W^+ + \bar{b}(p_2) + W^-, \quad (1)$$

[1] Our calculations are "exact" in the sense that we include gluon radiation off all colored particles in the production and decay process. Our only approximation is to assume that the gluon is "soft," i.e., $E_g/E \ll 1$, where $E \sim m_t$ is a typical energy scale of the subprocess.

where $ab = q\bar{q}$ or gg, and the particles' momenta are indicated in parentheses. Naively, the invariant mass of each b-W system is equal to m_t. Now suppose that the final state contains an extra gluon, with momentum k^μ. In terms of Feynman diagrams, this gluon can be emitted off (taking the $q\bar{q}$ process as an example) either of the incoming light quarks, the s-channel gluon, off either of the top quarks before they decay weakly (i.e., on the time scale of the strong production process), off either of the top quarks on the time scale of their weak decay, or off either of the final-state b quarks (and also from the decay products of a hadronically decaying W). All of these amplitudes can of course interfere.

Because of the infrared divergence associated with gluon emission, an extra jet in a $t\bar{t}$ event will usually be soft. In this case, one can analyze the radiation pattern in the soft gluon approximation, as was done in Refs. [2, 3]. One can write

$$\frac{1}{d\sigma_0}\frac{d\sigma}{dE_g\,d\cos\theta_g\,d\phi_g} = \frac{\alpha_s}{4\pi^2}\,E_g\,\mathcal{F}\,, \qquad (2)$$

where $d\sigma_0$ is the differential cross section for the lowest-order process (i.e., with no gluon radiation), E_g is the

energy of the soft gluon, and α_s is the strong coupling. The function $\mathcal{F}$ is the sum of "antenna patterns" of the radiation from the different sources listed above. It can be written generically as

$$\mathcal{F} = \mathcal{F}_{\text{prod}} + \mathcal{F}_{\text{dec}} + \mathcal{F}_{\text{int}}\,, \qquad (3)$$

where $\mathcal{F}_{\text{prod}}$ is the contribution from emission at the $t\bar{t}$ production stage (including initial-state radiation), $\mathcal{F}_{\text{dec}}$ is the contribution from emission off the t and $\bar{t}$ and their decay products at the weak decay stage, and $\mathcal{F}_{\text{int}}$ refers to the interferences between these emissions. More specifically, $\mathcal{F}_{\text{int}}$ contains contributions from the interference (i) between radiation in the t decay and that in the $\bar{t}$ decay and (ii) between radiation in $t\bar{t}$ production and radiation in either decay.[2] Note that for soft gluons with $E_g \sim \Gamma_t \sim 1$ GeV, $\mathcal{F}_{\text{int}}$ is sensitive to the top decay width, as discussed in Ref. [2]. However, the observable soft jets that are relevant to the $p\bar{p}$ collider experiments have energies much larger than Γ_t, and so in practice the interference terms are numerically small.

Explicit expressions for $\mathcal{F}$ for the $q\bar{q}$ and gg subprocesses have been presented in [3] and are listed again here for completeness:

$$\mathcal{F}_{\text{prod}} = c_1\widehat{k_1k_2} + c_2\widehat{k_1q_1} + c_3\widehat{k_1q_2} + c_4\widehat{k_2q_1} + c_5\widehat{k_2q_2} + c_6\widehat{q_1q_2} + c_7\widehat{q_1q_1} + c_8\widehat{q_2q_2}\,,$$

$$\mathcal{F}_{\text{dec}} = c_7[\widehat{q_1q_1} + \widehat{p_1p_1} - 2\widehat{q_1p_1}] + c_8[\widehat{q_2q_2} + \widehat{p_2p_2} - 2\widehat{q_2p_2}]\,,$$

$$\mathcal{F}_{\text{int}} = \chi_1\left\{c_2[\widehat{k_1p_1} - \widehat{k_1q_1}] + c_4[\widehat{k_2p_1} - \widehat{k_2q_1}] + c_6[\widehat{q_2p_1} - \widehat{q_1q_2}] + 2c_7[\widehat{q_1p_1} - \widehat{q_1q_1}]\right\}$$

$$+ \chi_2\left\{c_3[\widehat{k_1p_2} - \widehat{k_1q_2}] + c_5[\widehat{k_2p_2} - \widehat{k_2q_2}] + c_6[\widehat{q_1p_2} - \widehat{q_1q_2}] + 2c_8[\widehat{q_2p_2} - \widehat{q_2q_2}]\right\}$$

$$+ \chi_{12}\,c_6[\widehat{p_1p_2} - \widehat{q_1p_2} - \widehat{q_2p_1} + \widehat{q_1q_2}]\,, \qquad (4)$$

where the antennae $\widehat{pq}$ and "profile functions" χ_i are defined by

$$\widehat{pq} = \frac{p\cdot q}{p\cdot k\, q\cdot k}\,,$$

$$\chi_i = \frac{m_t^2\Gamma_t^2}{(q_i\cdot k)^2 + m_t^2\Gamma_t^2}\quad (i=1,2)\,,$$

$$\chi_{12} = \frac{m_t^2\Gamma_t^2\,(q_1\cdot k\, q_2\cdot k + m_t^2\Gamma_t^2)}{[(q_1\cdot k)^2 + m_t^2\Gamma_t^2]\,[(q_2\cdot k)^2 + m_t^2\Gamma_t^2]}\,. \qquad (5)$$

In terms of the gluon energy, we have $\mathcal{F} \sim E_g^{-2}$, and so the cross section has the infrared behavior $d\sigma/dE_g \sim E_g^{-1}$, as expected. Additional collinear singularities arise from the $p\cdot k$ denominators when $p^2 = 0$.

The antenna coefficients c_i depend on the color structure of the hard scattering and are different for the $q\bar{q}$ and gg processes $(C_F = 4/3,\ N = 3)$:

Coefficient	$q\bar{q} \to t\bar{t}$	$gg \to t\bar{t}$
c_1	$-\frac{1}{N}$	$-2C_F + 2N + 2Y$
c_2	$2C_F - \frac{1}{N}$	$C_F - X - Y$
c_3	$\frac{2}{N}$	$C_F + X - Y$
c_4	$\frac{2}{N}$	$C_F + X - Y$
c_5	$2C_F - \frac{1}{N}$	$C_F - X - Y$
c_6	$-\frac{1}{N}$	$2Y$
c_7	$-C_F$	$-C_F$
c_8	$-C_F$	$-C_F$

The quantities X and Y depend on the $gg \to t\bar{t}$ subprocess energy and scattering angle. Explicit expressions and a discussion can be found in [3].

In general terms, the antennae which contribute to $\mathcal{F}_{\text{prod}}$ correspond to color strings stretched between the initial-state partons and the final-state t quarks before they decay, and those which contribute to $\mathcal{F}_{\text{dec}}$ correspond to color strings linking the final-state $t(\bar{t})$ and $b(\bar{b})$ quarks at the weak decay stage. We remind the reader that color antennae exhibit the "string effect:" radiation between the two momenta in an antenna is enhanced compared to that outside them; see, for example, Ref. [5]. We will see several instances below where this effect influences gluon distributions.

For purposes of top momentum reconstruction and mass measurement, this decomposition serves as a guide to what to do with additional soft jets from gluons. Gluons from the production stage are emitted before the t and $\bar{t}$ quarks go on shell and should not be included in top momentum reconstruction. Those from the decay

---

[2]In terms of the results of Ref. [2], $\mathcal{F}_{\text{prod}}$ corresponds to $|A|^2$, $\mathcal{F}_{\text{dec}}$ to $|B_1|^2 + |B_2|^2$, and $\mathcal{F}_{\text{int}}$ to $-2\text{Re}[B_1B_2^*] + 2\text{Re}[A(B_2 - B_1)^*]$.

stage *are* to be included along with the top decay products. For the interference contributions no such clearcut assignment is possible; however for the examples we consider here, the interference contribution is negligible.

B. Gluon radiation in simpler models

There are several simpler models which we could construct if we were interested in simulating gluon radiation in top events without using the full distribution, Eq. (4). Consider, for example, a model which includes only initial-state radiation (ISR). This would be appropriate, for example, for the purely electroweak process $q\bar{q} \to Z^0 \to l^+l^-$, where the color string is stretched between the incoming quarks. In the language of the antennae introduced above, this corresponds to

$$\mathcal{F} = 2C_F(2N)\,\widehat{k_1 k_2}\,, \tag{6}$$

for $q\bar{q}(gg) \to t\bar{t}$, respectively.

A more sophisticated approximation would also include final-state radiation (FSR) by allowing the b quarks to radiate, assuming that they were linked by a second color string, as, for example, for the process $q\bar{q} \to Z^0 \to b\bar{b}$. In this case we would find[3]

$$\mathcal{F} = 2C_F(2N)\,\widehat{k_1 k_2} + C_F\,[2\widehat{p_1 p_2} - \widehat{p_1 p_1} - \widehat{p_2 p_2}]\,. \tag{7}$$

We will refer to this model as ISR-FSR. The ISR and ISR-FSR models are easily implemented and are characteristic of what appears in parton-shower Monte Carlo simulations.

A third possible model corresponds to the naive expectation that the top quarks do not radiate because of their short lifetime. (In our case, where the relevant gluon energies are larger than Γ_t, the top quarks *do* radiate; see [2] for a discussion.) This model corresponds to taking $\Gamma_t \to \infty$ (and hence $\chi_i, \chi_{12} \to 1$) in Eq. (5) and gives

$$\mathcal{F} = c_1\widehat{k_1 k_2} + c_2\widehat{k_1 p_1} + c_3\widehat{k_1 p_2} + c_4\widehat{k_2 p_1} + c_5\widehat{k_2 p_2}$$
$$+ c_6\widehat{p_1 p_2} + c_7\widehat{p_1 p_1} + c_8\widehat{p_2 p_2}\,. \tag{8}$$

This is the radiation pattern we would see if the b and $\bar{b}$ were produced directly, and so we will refer to this model as BB.

In what follows, we will compare the complete distribution given in Eq. (4) with those from the ISR, ISR-FSR, and BB models, corresponding to Eqs. (6), (7), and (8).

III. NUMERICAL RESULTS AND DISCUSSION

In the previous section we have seen how the radiation pattern depends on the orientation of the final-state t and b quarks. This obviously varies from event to event, and in our calculations we must therefore integrate over

the full phase space for $t\bar{t}$ production and decay and weight by the appropriate parton distributions. This will then yield the correct radiation pattern in the laboratory frame. In particular, we will see important differences between the models discussed at the end of the previous section. To understand how and why these differences arise, it is helpful to first work in the parton subprocess center of mass, fixing the t and b momenta in "typical" configurations, as was done in Refs. [2, 3].

In order to assess the typical final-state configurations, we first generate a sample of events corresponding to $q\bar{q}, gg \to t\bar{t} \to b\bar{b}W^+W^- \to b\bar{b}ll\nu\nu$ with $m_t = 174$ GeV/c^2 and $m_b = 5$ GeV/c^2 in $p\bar{p}$ collisions at 1.8 TeV. Figure 1 shows the resulting distributions in $b(\bar{b})$ transverse momentum and pseudorapidity, and in the $b - \bar{b}$ azimuthal angle difference. The majority of b quarks are produced centrally (i.e., within $|\eta_b| < 1$) and with $p_T^b \sim 30 - 100$ GeV. The distribution in azimuthal angle difference shows a slight preference for back-to-back production in the transverse plane. We note for future reference that the centrality of the b's is due in large part to the fact that they receive a boost in the direction of their parent top quarks, which tend to be produced
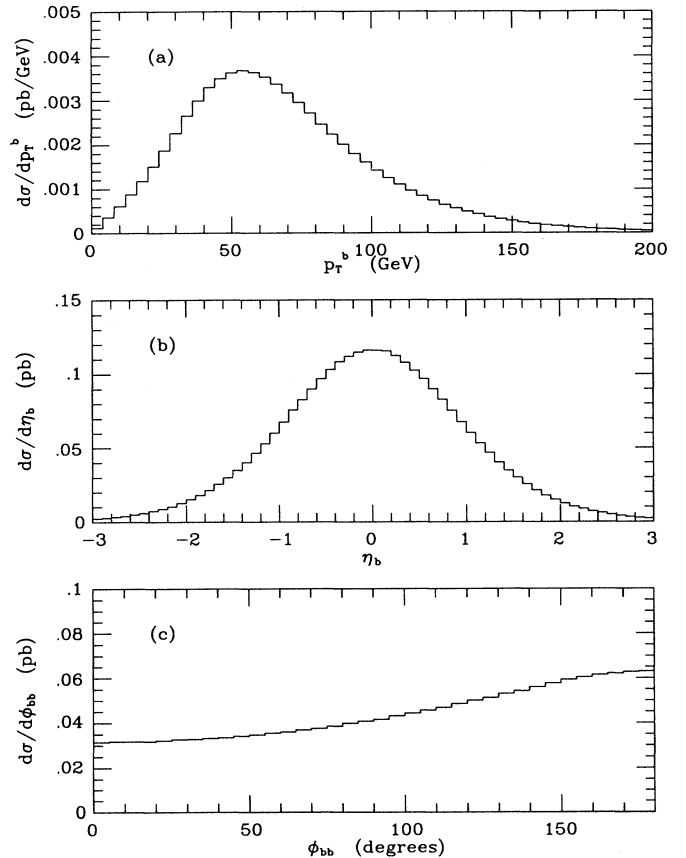

FIG. 1. Distributions in (a) the b-quark transverse momentum, (b) the b-quark pseudorapidity, and (c) the azimuthal angle difference between the b and $\bar{b}$ quarks, in $t\bar{t}$ production, via the subprocesses $q\bar{q}, gg \to t\bar{t} \to b\bar{b}W^+W^-$, in $p\bar{p}$ collisions at $\sqrt{s} = 1.8$ TeV.

---

[3]This would in fact be the correct result for the process $q\bar{q}(gg) \to H \to t\bar{t} \to b\bar{b}W^+W^-$ in the limit $\Gamma_t \to \infty$ [3].

centrally; this also accounts for their slight back-to-back preference. We note also that for $m_t = 174$ GeV/c^2, the cross section is dominated by the $q\bar{q} \to t\bar{t}$ process, which is an order of magnitude larger than the $gg \to t\bar{t}$ contribution.

A. Features of the gluon distribution in the $t\bar{t}$ center of mass

To investigate the radiation pattern of soft gluon emission, we choose a configuration with the following properties. For the moment we work in the $t\bar{t}$ center-of-mass frame, with subprocess energy $\sqrt{\hat{s}} = 3m_t$. The t and $\bar{t}$ are produced centrally ($\eta_t = \eta_{\bar{t}} = 0$) and the b quarks have $\eta_b = -\eta_{\bar{b}}$ and $\Delta\phi_{b\bar{b}} = 180°$, with the direction of the b defining $\phi = 0°$. For purposes of illustration, we will consider the particular case $\eta_b = 1$, which corresponds to $p_T^b = p_T^{\bar{b}} = 57$ GeV/c. The distribution of gluon radiation in the η-ϕ plane is then obtained from Eq. (2):

$$\frac{dN}{d\eta_g \, d\phi_g} \equiv \frac{1}{\cosh^2 \eta_g} \frac{1}{d\sigma_0} \frac{d\sigma}{dE_g \, d\cos\theta_g \, d\phi_g}$$
$$= \frac{\alpha_s}{4\pi^2} \frac{E_g \, \mathcal{F}}{\cosh^2 \eta_g} . \qquad (9)$$

At this stage we are only concerned with the general features of the radiation pattern, and so we (somewhat arbitrarily) set $E_g = 10$ GeV and $\alpha_s = 0.1$.

Figure 2 shows the distribution of Eq. (9), for the choice $\eta_b = 1$. The two most obvious features are (i) the strong enhancement of the radiation near the b and $\bar{b}$ directions, and (ii) the approximately constant "pedestal" distribution away from the b quark directions and in particular at large positive and negative η_g. Closer inspection reveals another important feature—*the radiation has minima close to the original t-quark directions*, in this case at $\eta_g \approx 0$. These represent the "dead cones" of the t and $\bar{t}$ quarks [2]. In order to study the various individual contributions to the distribution, and to compare different approximations, it is more useful to consider particular slices through the two-dimensional plot. In Fig. 3 we show the same distribution as a function of η_g for the

particular values $\phi_g = 0°$, $45°$, $90°$. The curves correspond to the decomposition of Eq. (4): the long-dashed line is the "production" contribution, the short-dashed line is the "decay" contribution, the dotted line is the interference contribution, and the solid line is the total. For $\phi_g(= \phi_b = \phi_t) = 0°$, we clearly see the dead cone of the b quark (in the decay contribution) and the much broader dead cone of the t quark (in the production contribution). The interference contribution is small. Away from the b-quark direction, the production contribution dominates. At $\phi_g = 45°$ the effects of the final-state quarks on the radiation pattern are much reduced, and at $\phi_g = 90°$, which is exactly half-way between the b and $\bar{b}$ quarks, the production contribution dominates and the distribution is approximately uniform.

Figure 4 shows the total contribution of Fig. 3 (solid line) compared to the distributions corresponding to the ISR (dashed line) and ISR-FSR (dotted line) models. The latter is approximately equal to the correct distribution close to the b-quark direction and at large forward and backward rapidities. However, it lacks the t-quark dead-cone effect, and overestimates the radiation in the region between the b and $\bar{b}$ quarks. The ISR model gives a constant contribution, and is in strong disagreement with the correct distribution for $|\eta_g| \lesssim 2$.

Although Figs. 3 and 4 are useful for illustrating particular features of the various models, they correspond to idealized situations where the momenta of the t and b quarks are fixed. In the next section, we present more realistic distributions corresponding to the fully integrated t- and b-quark cross sections.

B. Full gluon distributions in $t\bar{t}$ events at the Fermilab Tevatron

Here we obtain the full distribution of gluons expected in $t\bar{t}$ events at the Fermilab Tevatron, for the process $q\bar{q} \to t\bar{t} \to b\bar{b}W^+W^-$, with gluons generated according to Eq. (2). We use [Martin-Roberts-Stirling MRS(H)] parton distributions [4]. We neglect the $gg \to t\bar{t}$ process, whose contribution to the cross section is an
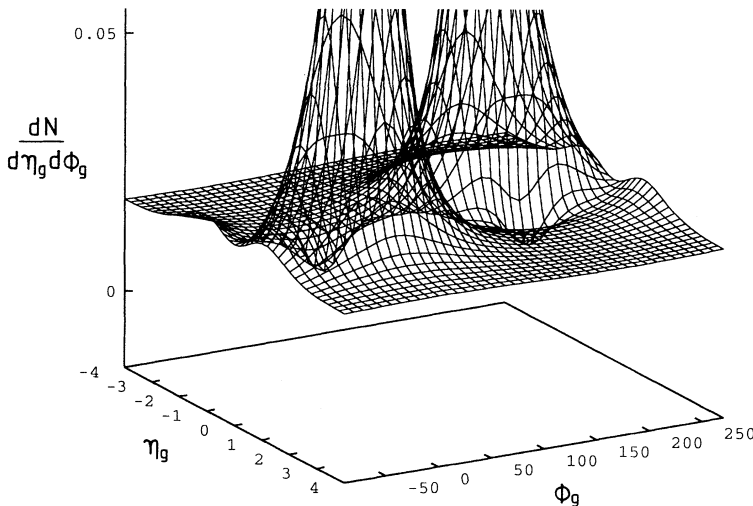

FIG. 2. Soft gluon radiation pattern in the η-ϕ plane, for the $q\bar{q} \to t\bar{t}$ process in the $t\bar{t}$ center-of-mass frame. The t, $\bar{t}$, and b, $\bar{b}$ quarks are at $(\eta, \phi) = (0, 0°)$, $(0, 180°)$ and $(\eta, \phi) = (1, 0°)$, $(-1, 180°)$, respectively.

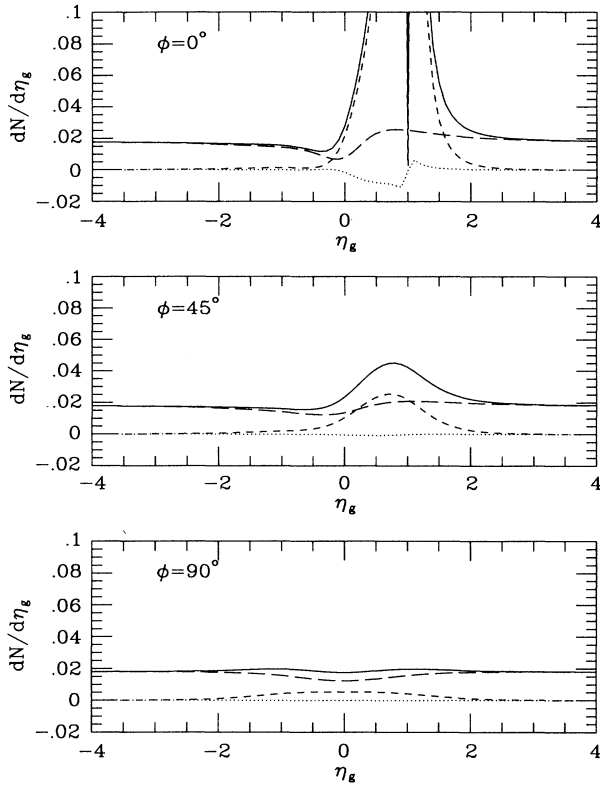FIG. 3. The soft gluon distribution of the previous figure for fixed values of ϕ_g. The curves correspond to the decomposition of Eq. (4): the long-dashed line is the "production" contribution, the short-dashed line is the "decay" contribution, the dotted line is the interference contribution, and the solid line is the total.

order of magnitude smaller than that for the $q\bar{q}$ initial state. This simplifies the interpretation of the results because the color structure of the two processes is different [3].

Our calculations are performed entirely at the parton level, and kinematic cuts are kept to a minimum. We require that the b's are produced centrally and that the gluons fall within some typical detector pseudorapidity range. We also require that the gluons have sufficient transverse momentum to be detectable as soft jets but not so much as to invalidate the soft approximation. Finally, we require some angular separation between the b's and gluons so that their respective jets are distinguishable. These requirements are implemented through the following kinematic cuts:

$$|\eta_b|, |\eta_{\bar{b}}| \leq 1.5 \,,$$
$$|\eta_g| \leq 3.5 \,,$$
$$10 \text{ GeV}/c \leq p_T^g \leq 25 \text{ GeV}/c \,,$$
$$E_g \leq 100 \text{ GeV} \,,$$
$$\Delta R_{bg}, \Delta R_{\bar{b}g} \geq 0.5 \,. \tag{10}$$

Note that the η_g cut eliminates the collinear singularities associated with initial-state radiation. With the exception of the cuts on ΔR and to some extent η_g, our results
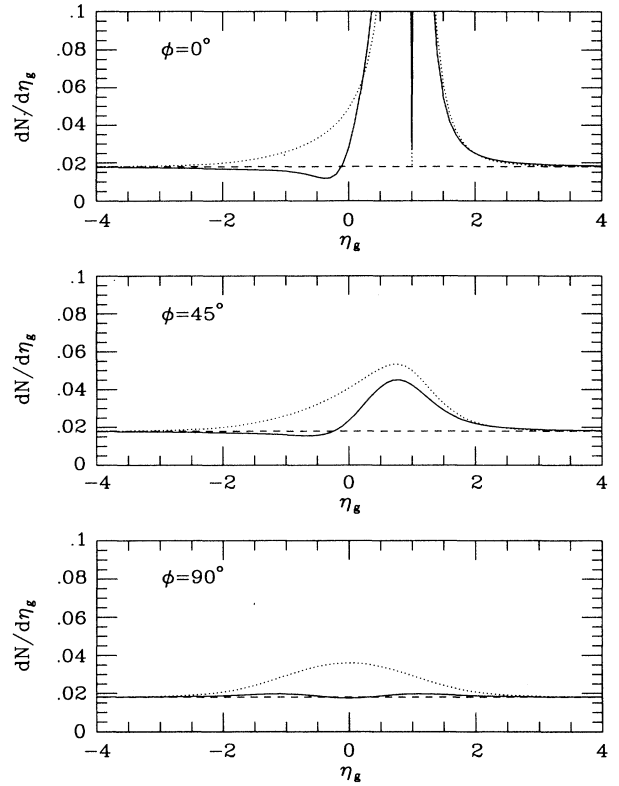
FIG. 4. The total soft gluon distribution of Fig. 3 (solid line) together with the distributions corresponding to the ISR (dashed line) and ISR-FSR (dotted line) models.

are not particularly sensitive to the exact values used.

Energy and transverse momentum distributions of the resulting gluons are shown as solid lines in Figs. 5(a) and 5(b). There are no surprises; the figures display the expected falloff with increasing energy and p_T, and reflect the lower and upper cutoffs. Also shown in Fig. 5 are the individual contributions according to the decomposition in Eq. (4), with contributions from production and decay appearing as dotted and dashed lines, respectively. The interference contribution is negligible for the energies considered here and is not shown in this plot or any that follow. We see that the energy distribution from the production piece extends to higher energies than that from decay, and that the decay p_T distribution is relatively flatter than that from production.

1. Angular distribution and top mass reconstruction

The difference between the distributions of gluons produced in the production and decay stages is displayed more dramatically in the gluon pseudorapidity distribution, Fig. 6. We are most interested in angular distributions in any case because we want to know where the soft jets are likely to appear in detectors. Figure 6 shows the net η_g distribution (solid line) along with the production-decay decompostion as in the previous figure. The decay contribution is peaked in the center and falls off quickly, whereas the production piece has a central
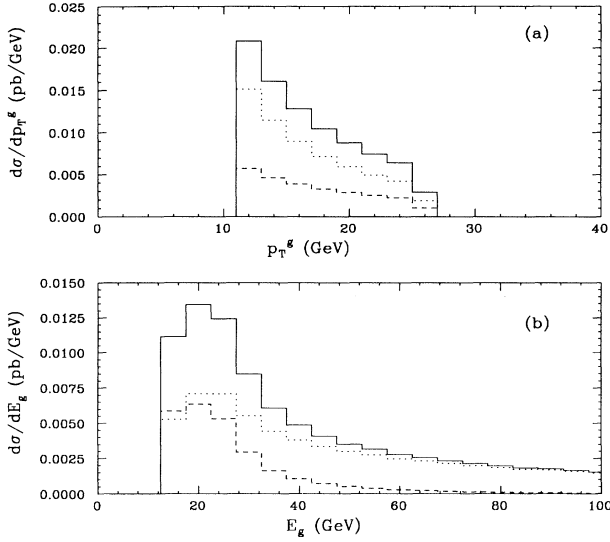
FIG. 5. Distributions in (a) the gluon energy and (b) the gluon transverse momentum, in $t\bar{t}$ production, via the subprocess $q\bar{q} \rightarrow t\bar{t} \rightarrow b\bar{b}W^+W^-$, in $p\bar{p}$ collisions at $\sqrt{s} = 1.8$ TeV. Contributions from production (dotted lines) and decay (dashed lines) are shown along with their totals (solid lines). The cuts are listed in Eq. (10).

dip and peaks in the forward direction. These results are easily understood when we consider the sources of the gluons; cf. Eq. (4). Gluons from the decay contribution come from radiation off the top and bottom quark lines. Radiation is largest near the quarks' direction of motion, and the quarks are, for the most part, produced centrally. Furthermore, we note that the string effect in the t-b and $\bar{t}$-$\bar{b}$ antenna pieces (the $\widehat{q_1 p_1}$ and $\widehat{q_2 p_2}$ terms in $\mathcal{F}_{dec}$) tends to enhance central radiation compared to that in the forward regions when the quarks are produced centrally. Similarly, the production piece arises from ra-
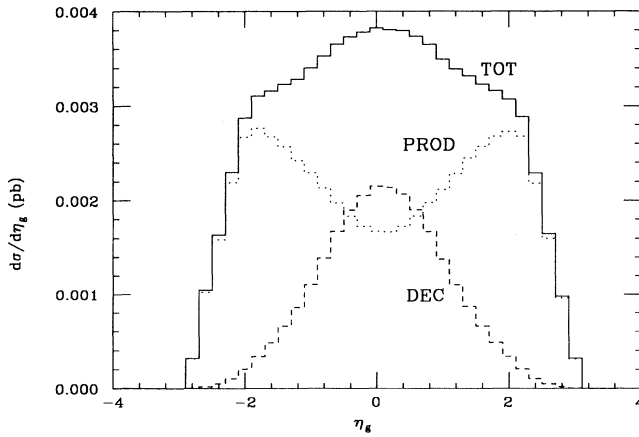
diation off initial-state quarks and the t and $\bar{t}$, and we get enhancement in the forward direction. The net effect is a total distribution that is slightly peaked in the center and falls off sharply above $\eta_g = 2$ or so.

Let us now compare these distributions with what we obtain using the simpler models described above. It seems plausible that the ISR-FSR model (initial-state and final-state radiation only, assuming color singlet initial and final states) would give a reasonable approximation to the correct distribution, with ISR corresponding to the production piece and FSR corresponding to decay. Figure 7 shows net η_g distributions for the various models, with the solid line again indicating the correct distribution according to Eq. (4). We see that the ISR model gives the flat rapidity distribution characteristic of initial-state radiation. Comparison with the production contribution in Fig. 6 (note the difference in vertical scales) shows that the ISR model significantly overestimates the amount of radiation in the central region. Adding to that radiation off the final b's to obtain the ISR-FSR distribution (dashed lines) leads to an even greater overestimate. Hence the ISR-FSR model is not a particularly good approximation to the full prediction: the overall normalization is too large and the total shape is wrong, being too strongly peaked in the center.

The other simple model, the BB model, in which the radiation is treated as in the direct $b\bar{b}$ production process $q\bar{q} \rightarrow b\bar{b}$, does in fact reproduce the net η_g distribution reasonably well; see the dot-dashed line in Fig. 7. Despite the fact that, for the gluon energies of interest here, the top width Γ_t can be considered to be small, the $\Gamma_t \rightarrow \infty$ limit seems to yield a good approximation to the full prediction; i.e., the results seem to be independent of the χ_i and χ_{12} factors in Eq. (4). The reason for this is related to the fact that radiation close to the b quarks is universal, independent of the process (see Ref. [3] for a discussion). But this result is deceptive for a number of reasons. First, depending as it does on radiation near

FIG. 6. Gluon pseudorapidity distributions in $t\bar{t}$ production, via the subprocess $q\bar{q} \rightarrow t\bar{t} \rightarrow b\bar{b}W^+W^-$, in $p\bar{p}$ collisions at $\sqrt{s} = 1.8$ TeV. The net distribution is shown as a solid line; contributions from production (dotted lines) and decay (dashed lines) are also shown. The cuts are listed in Eq. (10).
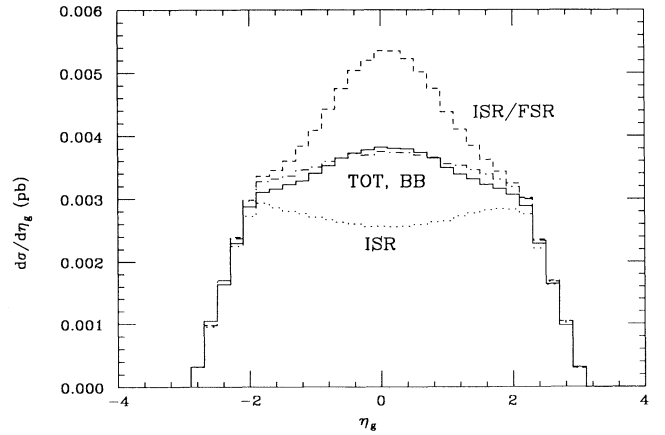

FIG. 7. Gluon pseudorapidity distributions in $t\bar{t}$ production, for the models discussed in Sec. II: full distribution (solid line), ISR model (dotted line), ISR-FSR model (dashed line), and BB model (dash-dotted line). The cuts are listed in Eq. (10).

the b's, it is sensitive to our choice of ΔR cut; if the gluons are restricted to be farther away from the b's, the agreement deteriorates. More important, although the η distribution seems to be well reproduced, the distribution in azimuthal angle is not, as we shall see below. Finally, because radiation off the t quarks is ignored, there is no way to decompose the results into production and decay contributions.

We now address the question, "What should be done with extra soft jets in attempts to reconstruct the top quark four-momentum?" As stated above, the decomposition of the gluon distributions into contributions from gluons radiated in top production and those radiated in decay provides guidance. Whether additional gluons in $t\bar{t}$ events should be combined with the b and W depends on what stage they are associated with: production gluons should not be combined, and decay gluons should. In principle there is also a contribution from interference terms which cannot be definitely associate with either stage, but in practice, for gluons sufficiently energetic to be identified as soft jets, these interference terms are negligible.

With this in mind, we return to the decomposition of the gluon pseudorapidity distribution shown in Fig. 6. We saw that gluons in the forward region are much more likely to have come from the production than the decay stage. Hence most forward gluons do not contribute to the top momentum, and based on these parton-level results it seems safe to conclude that soft jets with $|\eta_g| > 1.5$ can be ignored without introducing large systematic errors into the mass measurement. (This assumes, of course, that such jets are correctly identified.) Unfortunately the situation is less clearcut in the central region. Despite the central suppression of production-stage gluons, Fig. 6 shows that gluons in the central region are almost as likely to have come from production as from decay; in fact, with a larger ΔR cut, central gluons would be dominated by production. Note that the situation is even worse for the simpler models, since the ISR η_g distribution is flat, and the BB model allows for no decomposition at all.

In an attempt to identify a quantity that shows a clear excess in the decay contribution, we consider proximity to the b or $\bar{b}$ quark. It is certainly plausible to expect that soft jets near the b's are likely to have come from decay-stage gluons. Figure 8(a) shows the gluon distribution as a function of the cosine of the angle between the b and g, with the usual decomposition into production and decay contributions (dots and dashes, respectively), and total (solid). The production piece is flat, as expected since there is no dependence on the b direction in $\mathcal{F}_{\text{prod}}$, and the decay piece increases as the gluon approaches the b. At first sight this looks promising—there is an excess in the decay piece near the b. However, this result should not be taken quite at face value because the amount of this excess is extremely sensitive to the cuts, especially that on ΔR between the gluon and b. The excess can be reduced or even eliminated by reducing the gluon p_T range or increasing the ΔR cut. This would be compounded in practice by fragmentation of the partons into hadrons.

We can improve the situation by taking advantage of the difference in the production and decay pseudorapidity distributions and making a tighter η_g cut to eliminate much of the production contribution while retaining almost all of that from decay. Figure 8(b) shows that requiring $|\eta_g| \leq 1.5$ does indeed enhance the latter—the excess in the region near the b quark is now more pronounced. Unfortunately, the same caveats about cuts and fragmentation apply here, and we cannot safely quantify this excess or draw any firm conclusions.

It is clear from what we have seen above that assignments of soft jets to the production or decay stages cannot be made unambiguously on an event-by-event basis. However, we can minimize errors associated with soft jet ambiguities if we know what to expect from the correct gluon distribution and its decomposition and include it in our simulations. Eventually we may hope to find additional discriminators that improve the chances of making correct assignments, leading ultimately to a useful prescription for dealing with soft jets. The results shown here represent a first step in that direction. We do not perform mass reconstruction simulations here, since we do not use exact kinematics in the soft gluon approximation. In future work we intend to dispense with the soft
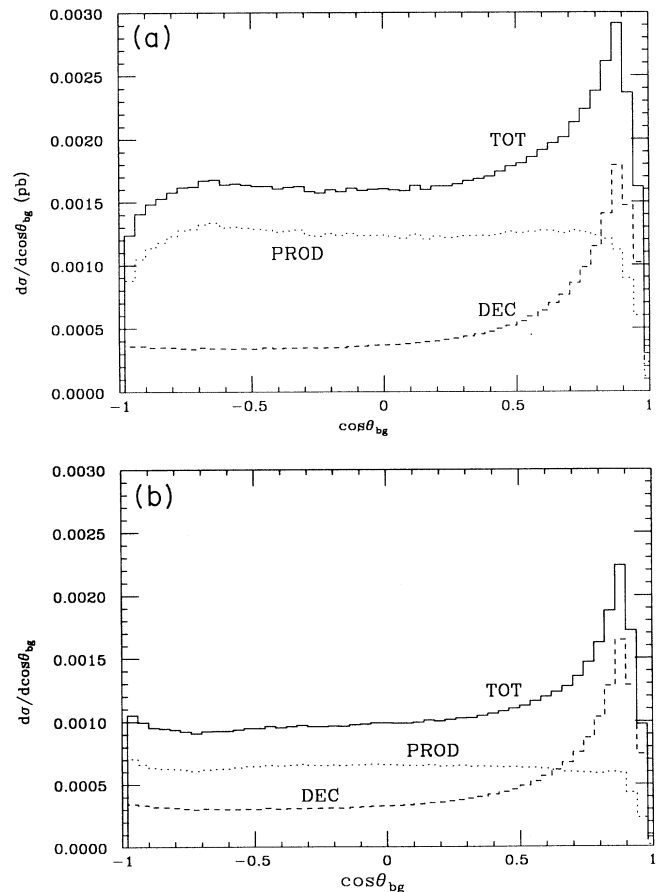
FIG. 8. Distribution in the cosine of the angle between the gluon and the b quark, (a) with cuts as in Eq. (10) and (b) with the additional cut $|\eta_g| \leq 1.5$.

approximation and perform the exact calculation, which will allow us to investigate more specifically issues associated with mass reconstruction.

2. Forward-backward asymmetry and color structure

We close this section by noting that the color structure of the process $q\bar{q} \to t\bar{t} \to b\bar{b}W^+W^-$ can give rise to distinctive effects in the gluon radiation pattern that can be explored experimentally, at least in principle. In particular, a forward-backward asymmetry appears in the distribution of gluons for an appropriately chosen class of final-state configurations. While not directly relevant to top mass measurement, this asymmetry helps to illuminate further some of the physics involved, for example the fact that the top quarks themselves can radiate gluons.

This asymmetry arises as a consequence of the string effects in the various antennae, that is, the enhancement of radiation between two quarks connected by a color string [6] (see also [5]). For example, in $q\bar{q} \to t\bar{t}$ the $\widehat{qt}$ antenna produces more radiation in the region between the t and q than, say, between the t and $\bar{q}$. This gives rise to a forward-backward asymmetry in the gluon radiation. This asymmetry is canceled in the net distribution by the $\widehat{\bar{q}t}$ antenna, of course. However, with suitably chosen cuts we can enhance one contribution (from radiation off the t, say) while suppressing the other, thereby recovering the asymmetry. We do this by taking advantage of the fact that there is more radiation from a quark in the regions nearby than those far away.

Guided also by the fact that the directions of the b quarks' momenta tend not to be too different from those of their parent t's, we add to the event selection criteria of Eq. (10) the requirement that the separation in azimuthal angle between the b and $\bar{b}$ be greater than $135°$. This tends to select events in which the parent t and $\bar{t}$ have similar separation. We then preferentially select gluons associated with the t (as opposed to the $\bar{t}$) by requiring that they lie within $90°$ in azimuth of the b quark. Figure 9(a) shows the resulting distribution as a solid line. A clear excess is visible in the forward direction, which is the directions of the initial quark's momentum. An equal and opposite asymmetry is obtained by considering gluons within $90°$ of azimuth of the $\bar{b}$.

That the source of this asymmetry is indeed the terms involving the initial quark and the t and $\bar{t}$ [cf. Eq. (4)] can be seen from the decomposition shown in Fig. 9(a), where, as in earlier figures, the production contribution is shown as the dotted line and the decay contribution is the dashed line. We see that the entire asymmetry comes from the production piece. The decay piece involves only the top and bottom momenta and there is no correlation with the initial quarks.

Finally, the asymmetry distribution reveals major discrepancies between the correct distribution and all three of the simpler models, as shown in Fig. 9(b). In the ISR (dotted line) and ISR-FSR (dashed line) models, in which there is no connection between radiation from the initial and final states, there can be no forward-backward asym-
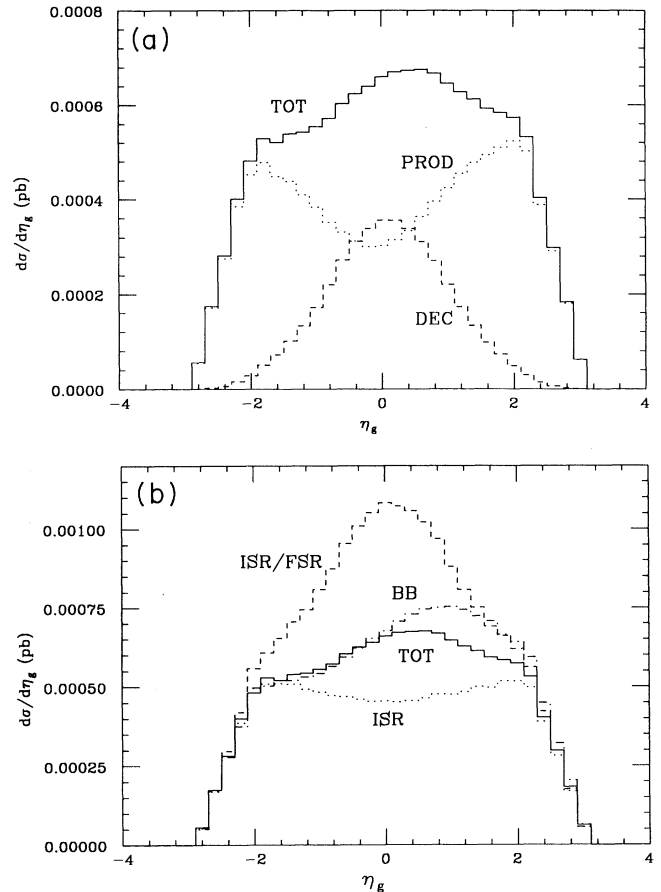

FIG. 9. Forward-backward asymmetry in gluon pseudorapidity distributions in $t\bar{t}$ production. The cuts are as in Eq. (10) with the additional requirements $\Delta\phi_{b\bar{b}} > 135°$ and $\Delta\phi_{bg} < 90°$. The curves correspond to the (a) total (solid), production (dots) and decay (dashes) distributions, and to the distributions for the (b) full QCD (solid), ISR (dots), ISR-FSR (dashes), and BB (dash-dotted) models.

metry. In contrast, the BB model has a more pronounced asymmetry even than the correct distribution because, without radiation from the top quarks, the antennae connecting initial- and final-state quarks are enhanced. This difference between BB and the correct result shows that the BB model does not contain the correct azimuthal dependence, despite the fact that it appears to reproduce the correct total η_g distribution in Fig. 7.

IV. CONCLUSIONS

The pattern of soft gluon radiation in $t\bar{t}$ production in hadronic collisions has a very rich structure. The initial-state partons, the t and b quarks can all radiate, and the gluon distribution in any part of phase space is a combination of what can be termed "production," "decay," and "interference" contributions. Apart from providing some interesting tests of the color structure of the events, there are important implications for top mass measurements from the invariant mass of the decay products. In

this study we have attempted to illustrate the general features of the radiation pattern. We have quantified the idea that soft jets close to the b quarks can be associated with gluon emission in the top decay process, while radiation at large rapidities can be associated with radiation at the $t\bar{t}$ production stage. We have compared the full QCD prediction with those of simpler models, which are characteristic of how radiation may be implemented in Monte Carlo event generators. It is not difficult to find regions of phase space where the models differ significantly from the full prediction. Our conclusion is that the question of how to handle additional soft jets in $t\bar{t}$ events when reconstructing the top momentum is far from trivial. In a future study we intend to go beyond the soft gluon approximation to study the invariant mass distributions themselves.

ACKNOWLEDGMENTS

[1] CDF Collaboration, F. Abe *et al.*, Phys. Rev. D **50**, 2966 (1994).

[2] V.A. Khoze, L.H. Orr, and W.J. Stirling, Nucl. Phys. **B378**, 413 (1992).

[3] V.A. Khoze, J. Ohnemus, and W.J. Stirling, Phys. Rev. D **49**, 1237 (1994).

[4] A.D. Martin, R.G. Roberts, and W.J. Stirling, in *Proceedings of the Workshop on Quantum Field Theoretical Aspects of High Energy Physics*, Kyffhäusser, Germany, edited by B. Geyer and E.-M. Ilgenfritz (Englemen, Leipzig, 1993), p. 11.

[5] Yu.L. Dokshitzer, V.A. Khoze, A.H. Mueller, and S.I. Troyan, *Basics of Perturbative QCD* (Editions Frontières, Gif-sur-Yvette, France, 1991).

[6] G. Marchesini and B.R. Webber, Nucl. Phys. **B330**, 261 (1990).